HIV viral protein R induces loss of DCT1-type renal tubules

Khun Zaw Latt, Teruhiko Yoshida, Shashi Shrivastav, Amin Abedini, Jeff M. Reece, Zeguo Sun, Hewang Lee, Koji Okamoto, Pradeep Dagur, Jurgen Heymann, Yongmei Zhao, Joon-Yong Chung, Stephen Hewitt, Pedro A. Jose, Kim Lee, John Cijiang He, Cheryl A. Winkler, Mark A. Knepper, Tomoshige Kino, Avi Z. Rosenberg, Katalin Susztak, Jeffrey B. Kopp

Supplementary Materials

Supplementary Methods

Generation and maintenance of Vpr transgenic mice

PEPCK/tTA (T8 line) mice were crossed with tet-op/Vpr mice (L2 line) to generate dual-transgenic mice (Vpr Tg mice). Seven-to-nine week old female WT and Vpr Tg mice were maintained on a diet containing doxycycline (TD 98186, Envigo, Madison, WI) to inhibit the expression of Vpr. Mice were switched from doxycycline diet to 65% protein food (TD 190088, Envigo) for two weeks to induce transgene promoter activity. Both WT and Vpr Tg mice were fed with freshly prepared semi-solid sodium-deficient food [TD 90228 (3 g), containing casein (33.3%), agar (0.5%), sodium (0.045%), and 2.67 mL of water] for four days.(1, 2) Two WT FVB/N mice maintained on regular laboratory chow were also included for comparison. The mouse experimental protocol was approved in advance by the NIDDK Animal Care and Use Committee.

Tissue microarray preparation

Seven WT and thirteen Vpr Tg mouse kidney tissues were fixed with 10% buffered formalin for 24 hours, stored in 70% ethanol, and embedded in paraffin. Tissue microarrays (TMAs) containing 5 μm sections of kidney cortex tissues of WT and Vpr Tg mice were prepared at the Experimental Pathology Laboratory, Laboratory of Pathology, Center for Cancer Research, NCI, NIH. Triplicate cortex samples from seven WT and thirteen Vpr Tg mice were placed on the TMA slides. *In situ* hybridization, immunohistochemistry (IHC) and tunnel assay were performed on the TMA slides, as described below.

In situ hybridization

Fluorescence *in situ* hybridization was performed on TMAs using RNAscope reagents (Advanced Cell Diagnostics, Bio-techne, Minneapolis, MN). Briefly, the TMA slides were de-paraffinized, boiled with RNAscope target retrieval reagent for 15 min and digested with protease at 40 °C for 30 min. This was followed by hybridization for 2 h at 40 °C with RNA probes against *Pvalb* and *Slc12a3*. In addition, *Slc8a1*, *Trpv5* and *Hipk2* were also tested. Specific probe binding sites were visualized using fluorescent RNAscope Hiplex12 Reagents Kit (488, 550, 650) v2 (Catalog # 324419, Advanced Cell Diagnostics).

Immunohistochemistry (IHC) of parvalbumin

Tissue microarray slides were deparaffinized and rehydrated; antigen retrieval was performed by treating with citrate-buffered medium for 15 min in a hot water bath. The tissue samples were blocked with 2.5% normal horse serum for 20 min. The sections were incubated for 1 h at room temperature with the primary antibody against DCT1-specific parvalbumin (ab11427, 1 μg/ml, Abcam, Cambridge, UK) which was detected with the ImmPRESS HRP Universal Antibody (horse anti-mouse/rabbit IgG) Polymer Detection Kit and ImmPACT DAB EqV Peroxidase (HRP) Substrate (Vector Laboratories, Burlingame, CA) protocol, and counter stained with hematoxylin.

Tunnel assay to detect apoptotic cells

Terminal deoxynucleotidyl transferase dUTP nick end labeling (TUNEL) was used for detecting DNA fragments generated during apoptosis. Tunnel assay on TMA was performed by Histoserve (Germantown, MD).

Quantification of IHC and TUNEL images

Stained TMA slides were scanned at 40x on a Hamamatsu Nanozoomer. Using QuPATH (0.3.2), TMA masks were generated following color normalization and tissue detection. For paravalbumin detection, annotation masks for paravalbumin positive and negative tubular profiles were established to allow for automated detection. Percent parvalbumin-positive tubular area (mm^2) was calculated as percent of cortical area. For TUNEL quantification, nuclei were segmented and a threshold set for TUNEL positive nuclei, percentage of TUNEL-positive nuclei was calculated.

Confocal microscopy & image analysis

A Yokogawa CSU-W1 SoRa spinning disk confocal scan head (Yokogawa, Sugar Land, TX), with 50 micron pinhole (standard confocal mode, no SoRa), mounted on a Nikon Ti2 microscope (Tokyo, Japan). NIS-elements 5.21.02 imaging software (Nikon Instruments, Melville, NY), was used to collect tiles of multi-color fluorescence images. Fluorescence image channels were obtained sequentially, while sharing the Yokogawa T405/488/568/647 dichroic beamspitter.

DAPI fluorescence was excited by the 405nm laser and emission was filtered by ET455/58 (Chroma, Technology Corp, Bellows Falls, VT). Green fluorescence was excited by the 488nm laser and emission was filtered by ET520/40 (Chroma). Orange fluorescence was excited by the 561nm laser and emission was filtered by ET605/52 (Chroma). Far red fluorescence was excited by the 640nm laser and emission was filtered by ET655LP (Chroma). Images used for quantitation of stain prevalence were acquired with the Nikon Plan-Apoλ 20x/0.75 objective lens, producing a confocal section thickness of 7-7.5μm for all fluorescence channels. Whenever images of the same channel were to be compared during analysis, the same settings were used for acquisition.

For pre-processing images, NIS Elements was used to stitch, align, crop, and denoise (AI.denoise) images, followed by export to OME TIF for further processing. Fiji software(3) protocol used to quantify secondary antibody fluorescence occurring in each TMA spot was as follows: 1) Spot ROIs (Regions of Interest) were defined manually to exclude dust and any other potential areas of artifact, and also including an appropriate area around the spot for the auto-thresholds to work properly; 2) Relevant signal area, determined by Triangle threshold, was determined; 3) Nuclear area was determined by Otsu threshold, removing unrealistically small size nuclei from the threshold mask; 4) Signal area calculated above was normalized to tissue area by dividing by nuclear area. Macros were used to facilitate the protocol. For presentation, images were contrast-enhanced, by the same amount when comparing different conditions.

Fiji software was used for generating measurements for each TMA spot, which were copied to a spreadsheet for calculating (Total signal area) / (Total nuclear area).

1. The multi-channel OME TIF images were loaded into Fiji, one TMA at a time. To conserve memory, the BioFormats plugin was used to limit the channels loaded to those

that were currently needed, i.e. the two channels representing the nuclear stain and the signal of interest.

2. A ROI (Region Of Interest) was defined for every spot.
    a. The spot was zoomed to fill the computer monitor, on both channels, to identify and avoid potential artifacts when drawing the ROI. The channel acquired with UV or violet excitation, which is also the channel used to label nuclei in this paper, was particularly useful at revealing contaminant (and autofluorescent) dust.
    b. If the spot was mostly circular and free of artifacts; then a circle was used to define the ROI; otherwise, a polygon, to avoid the artifacts..
    c. ROIs were generally slightly larger than spot boundaries, without forgetting that too many non-biological pixels in the ROI could potentially cause problems later with auto-thresholding.
3. ROI Manager was used to organize the list of ROIs for each TMA, which could be saved for later use, and edited if needed. For convenience, the names of the ROIs were defined according to row and column number, e.g. R1C1, and sorted alphabetically. ROI Manager is required for the two macros described below.

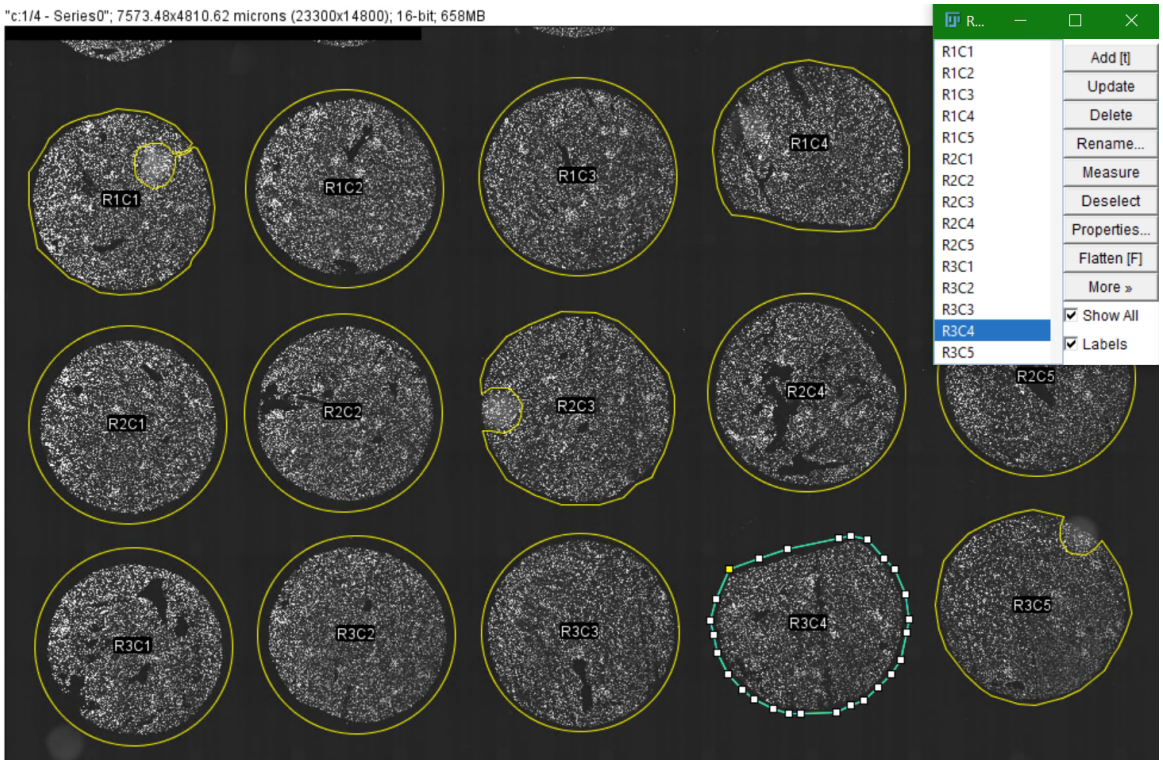

4. Macro "ROIManLoop_Thresh-MeasureSigArea.ijm" measures the total area (in sq. microns) in each TMA spot where valid signal exists.
    a. The Triangle auto-threshold is used to define which pixels qualify as valid signal. The threshold is applied locally to each ROI, to account for deviations in background across the TMA.

```
// Macro ROIManLoop_Thresh-MeasureSigArea.ijm
// Purpose: loops through the ROIs in ROI Manager,
```

```
// ...measuring the area in each ROI that is above threshold (valid signal).
// NOTE: ROIs need to be defined in ROI Manager for this macro to work!!

waitForUser("Please make sure you have the image selected \n for MEASURING
AREA OF FLUORESCENCE SIGNAL, \n and \n ROI Manager has the right
ROI list.\n---> THEN Click OK or press the ENTER key to continue");
currimage=getTitle();
run("Set Measurements...", "area limit display redirect=None decimal=0");
// mean not used for analysis, but could be
Table.create("Results");  // clears Results table
run("Input/Output...", "jpeg=90 gif=-1 file=.csv save_column save_row");
// omitting column and row names for copying data from Results tables

n = roiManager("count");
for (i = 0; i < n; i++) {
   selectWindow(currimage);
   roiManager("select", i);
// Duplication not necessary for measuring, but useful for showing thresholds for
QC,
// plus threshold display is quicker on smaller images.
    RoiImage = Roi.getName+"_SigThr";
    run("Duplicate...", " ");
    setAutoThreshold("Triangle dark");
    // particular auto-threshold method is sample- and probe-dependent
    run("Measure");
    rename(RoiImage);
}
ResultsNewName = "Results for Fluorescence Signal in " + currimage;
Table.rename("Results", ResultsNewName);
run("Tile");
```

b. A cropped image of each spot, with threshold visualized, was generated along with its measurement. These spot-images provided a quick visual QC check, for two things: areas of artifact missed when defining the ROI earlier; and the actual threshold, whether it seems reasonable.
c. If there were any thresholded areas that looked like artifacts, missed during the previous step when defining ROIs, those ROIs could be adjusted.
d. If a spot's auto-threshold seemed to be conspicuously lower that what the viewer's common sense judgement would dictate for "valid signal", the ROI boundaries for those outlier spots are checked to see if too many non-biological background pixels were included. The Triangle threshold uses peaks in the histogram for determining the threshold; if there is measurable autofluorescence above the level of non-biological background, it should be the main source of the histogram peak, not the non-biological background.

e. If any adjustments were made to the ROIs, the ROI list was re-saved in ROI Manager, and the macro was re-run to generate new Results.
f. When the visual QC check is passed, the Results are copied to the spreadsheet that has been set up for analysis.

5. Macro "ROIManLoop_Thresh-MeasureNucArea.ijm" measures the total area (in sq. microns) in each TMA spot where nuclear signal exists.
    a. The Otsu auto-threshold was used to define which pixels qualify as nuclear signal. The threshold was applied locally to each ROI, to account for deviations in background across the TMA.

```
// Macro ROIManLoop_Thresh-MeasureNucArea.ijm
// Purpose: loops through the ROIs in ROI Manager,
// ...measuring the area in each ROI that is above threshold (valid nuclear signal).
// Analyze Particles is used to eliminate particles too small to be nuclei.
// NOTE: ROIs need to be defined in ROI Manager for this macro to work!!

waitForUser("Please make sure you have the image selected for MEASURING
NUCLEAR AREA, \n and \n ROI Manager has the right ROI list.\n---> THEN
Click OK or press the ENTER key to continue");
currimage=getTitle();
run("Set Measurements...", "area limit display redirect=None decimal=0");
run("Input/Output...", "jpeg=90 gif=-1 file=.csv save_column save_row");
// omitting column and row names for copying data from Results tables
Table.create("Summary");  // clears Summary table

n = roiManager("count");
for (i = 0; i < n; i++) {
   selectWindow(currimage);
    roiManager("select", i);
// Duplication not necessary for measuring, but useful for creating mask images
for QC
    RoiName = Roi.getName;
    run("Duplicate...", "title=[ROIduplicate]");
    rename(RoiName);
   setAutoThreshold("Otsu dark");
    run("Analyze Particles...", "size=10-Infinity show=Masks exclude clear
include summarize");
    NucMaskImage = RoiName+"_Nucmask";
    rename(NucMaskImage);
    close(RoiName);
}
LatestSummary = "Summary for "+currimage;
Table.rename("Summary", LatestSummary);
run("Tile");
```

b. A cropped image of each spot, converted to an inverted mask of thresholded nuclei, was created as a quick visual QC check.
c. If the nuclear masks (i.e. thresholds) looked reasonable, the Summary table was copied to the spreadsheet for analysis.

In vitro detection of apoptosis in Vpr-treated 209 mDCT cells

Caspases are *c*ysteine-*a*spartic acid-*s*pecific *p*rote*ases* that are activated in response to different cell death-inducing stimuli (1).Therefore, The CHEMICON CaspaTag™ Pan-Caspase *In Situ* Assay Kit (APT420, EMD Millipore) was used according to the manufacturer's protocol, with minor changes as described below to detect apoptosis induced in mDCT cells treated with sVpr.

The 209 mDCT cells (ATCC) were grown in DMEM containing 10% FBS and penicillin-streptomycin. For the assay, 10,000 cells /200 µl of culture medium were grown overnight in a 96-well plate. Next day, cells were treated with opti medium containing sVpr (1ng/200µl/well). The control well received Opti-MEM medium (Gibco) only. Twenty four hours later, the cells were stained with 1x FLICA for 1hour at 370C, then washed twice with 1x wash buffer provided with the kit. Cells were trypsinized with 50µl of 0.025% trypsin and neutrilized with 50µl of medium. Accutase (Cat.# 00-4555-56 Thermo Fisher) containing propidium iodide *(*PI 250ng/100µl accutase) was added, immediately before the FACS analysis. Cells were then viewed at excitation at 490nm, emission >520nm. PI has a maximum emission of 637nm.

Quantitive PCR of *Ier3* in 209 mDCT cells

Mouse 209 DCT cells (10^5 /ml) were grown overnight in six well plates. Next day, cells were treated with fresh medium containing 0.0. 0.1,10 and 100 ng/ml of sVpr for 24 hours. The RNA from control and Vpr-treated 209 mDCT cells were prepared by Tryzol (Sigma). The forward and reverse primers used for Ier3 amplification were: mmu-Ier3F ACACCTGAGCCCATTTCTG and mmu-Ier3-R TGACCCATCGCGTTTAGAAG, respectively. The values were normalized to beta-actin amplified using the following primers: mActb-F CCACCATGTACCCAGGCATT and mActb-R AGGGTGTAAAACGCAGCTCA.

Supplementary References

1. Balasubramanyam A, Mersmann H, Jahoor F, Phillips TM, Sekhar RV, Schubert U, et al. Effects of transgenic expression of HIV-1 Vpr on lipid and energy metabolism in mice. *Am J Physiol Endocrinol Metab.* 2007;292(1):E40-8.
2. Shrivastav S, Lee H, Okamoto K, Lu H, Yoshida T, Latt KZ, et al. HIV-1 Vpr suppresses expression of the thiazide-sensitive sodium chloride co-transporter in the distal convoluted tubule. *PLoS One.* 2022;17(9):e0273313.
3. Schindelin J, Arganda-Carreras I, Frise E, Kaynig V, Longair M, Pietzsch T, et al. Fiji: an open-source platform for biological-image analysis. *Nat Methods.* 2012;9(7):676-82.

Supplementary Figures

(a)

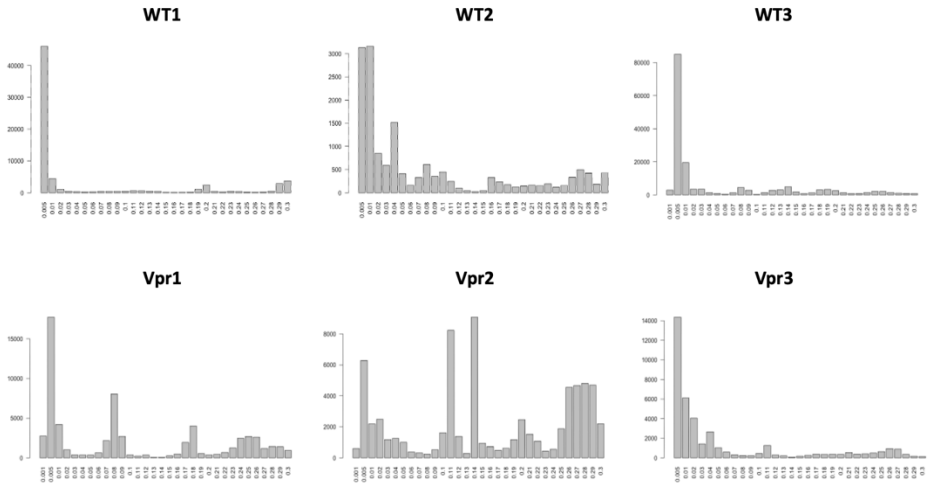

(b)

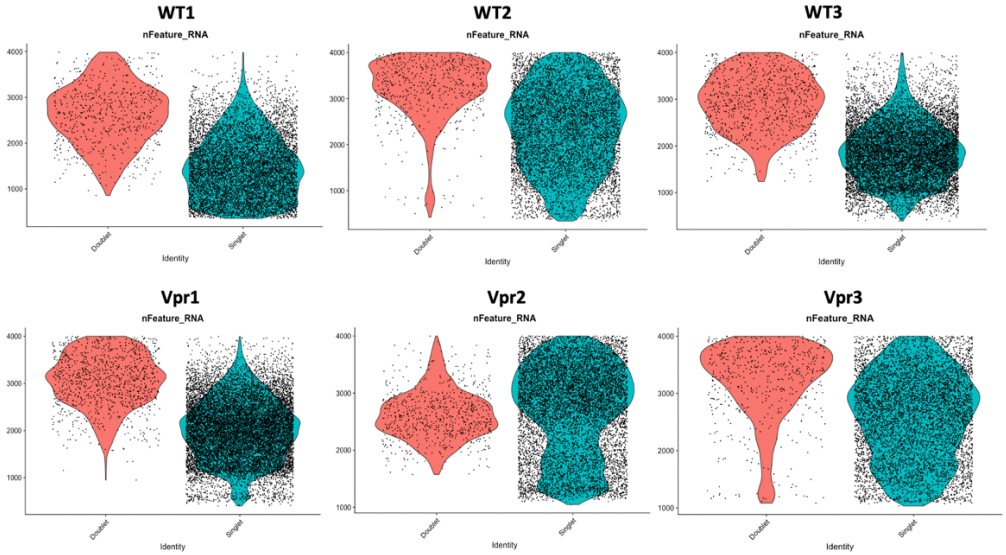

Supplementary Figure 1. Results of doublet detection analysis in each sample by DoubletFinder. (a) Barplots showing BC metrices (Y-axis) for different pK values (X-axis). (b) Violin plots showing the nFeature_RNA counts in predicted single and doublet samples.

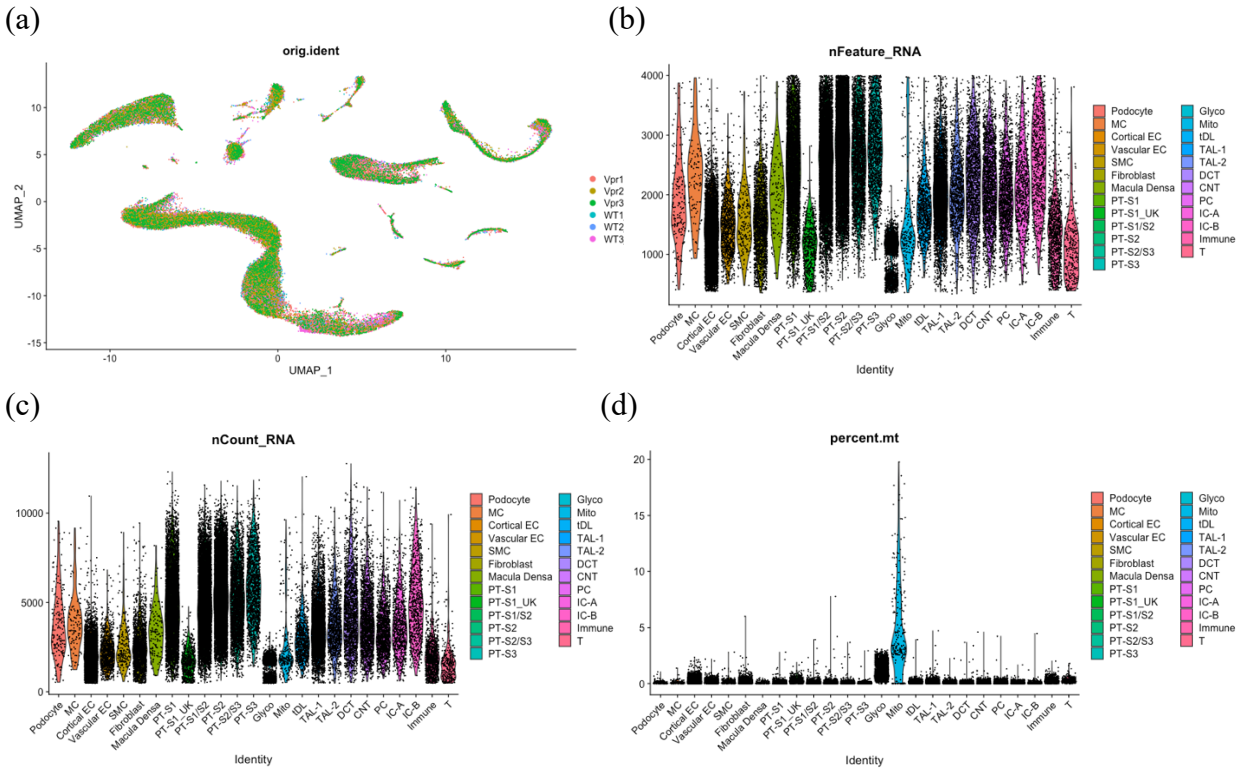

Supplementary Figure 2. snRNA-seq analysis of the dataset after anchor-based integration and batch correction by harmony. (a) UMAP of the merged dataset with original samples in different colors (b) Violin plot showing the number of features (genes) expressed in each cell in each cluster (c) Violin plot showing the total number of mRNA expressed in each cell in each cluster (d) Violin plot showing the percentage of mitochondrial transcripts in each cell in each cluster.

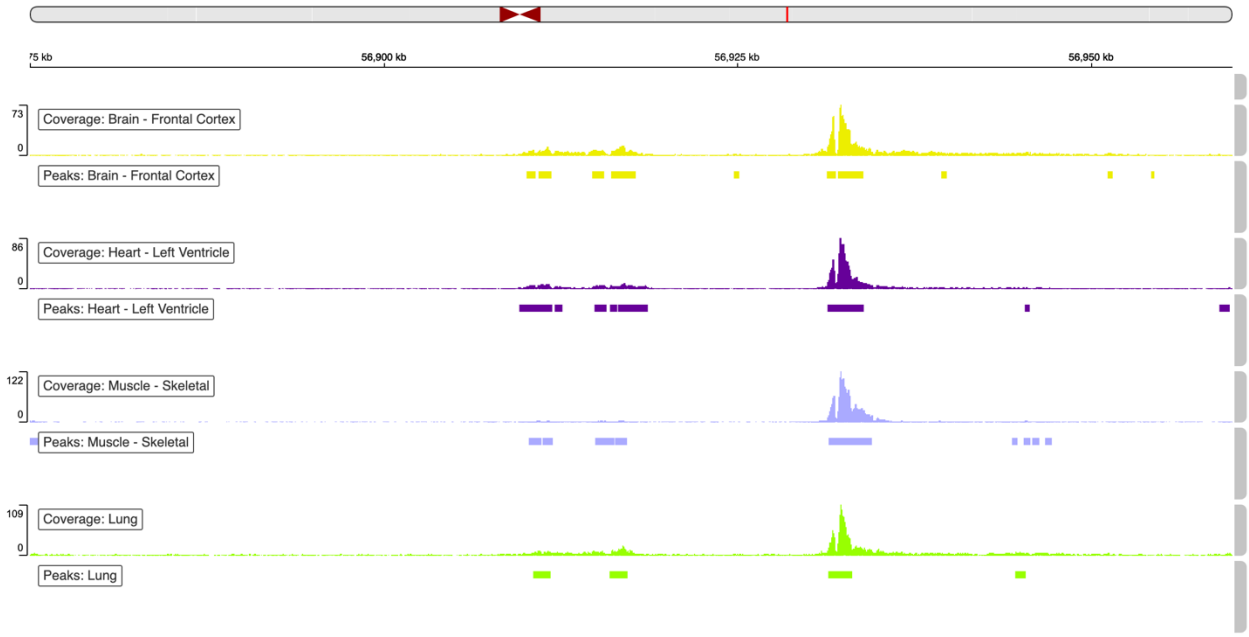

Supplementary Figure 3. H3K27ac enhancer mark on human chromosome 16 covering *SLC12A3* region in frontal cortex, left ventricle, skeletal muscle and lung retrieved from GTEx database.

(a)

(b)

Supplementary Figure 4. Candidate cis-regulatory elements (cCREs) in human SLC12A3 region retrieved from ENCODE database showing multiple enhancer-like elements (yellow vertical bars) in all registry samples. (a) DNase-seq signal in glomerular epithelial cells from two adult males (b) CTCF ChIP-seq signal in kidney tissues from three adult males.

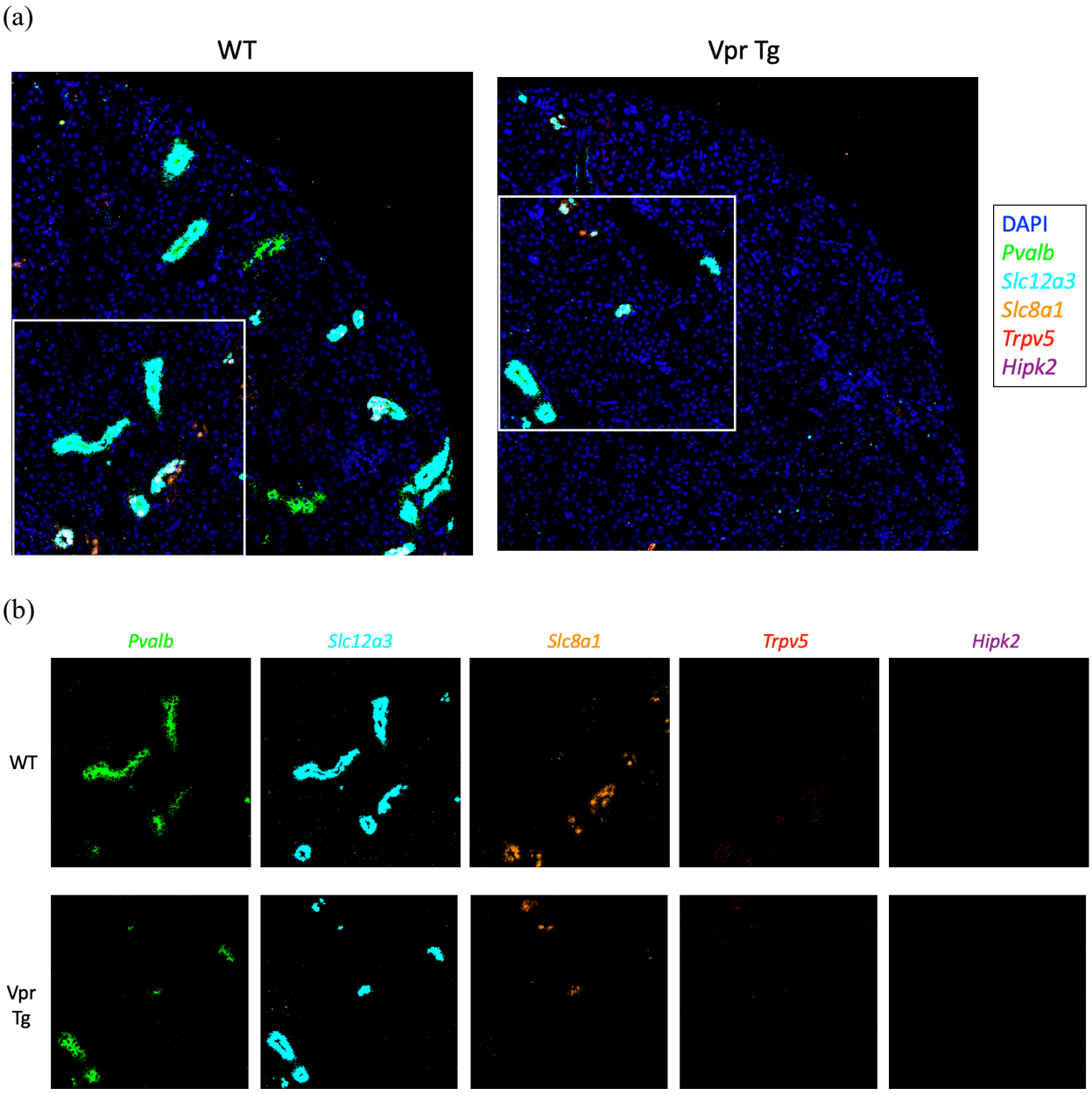

Supplementary Figure 5. Imaging results of WT and Vpr Tg cortex samples. (a) RNAScope images of the right upper quadrant of a tissue microarray section showed that compared to WT, Vpr Tg sample had less *Slc12a3* and *Pvalb* fluorescence signals. (b) Areas of images from figure (a) marked by the white rectangles shows individual genes for *Pvalb*, *Slc12a3*, *Slc8a1*, *Trpv5* and *Hipk2*.

(a)

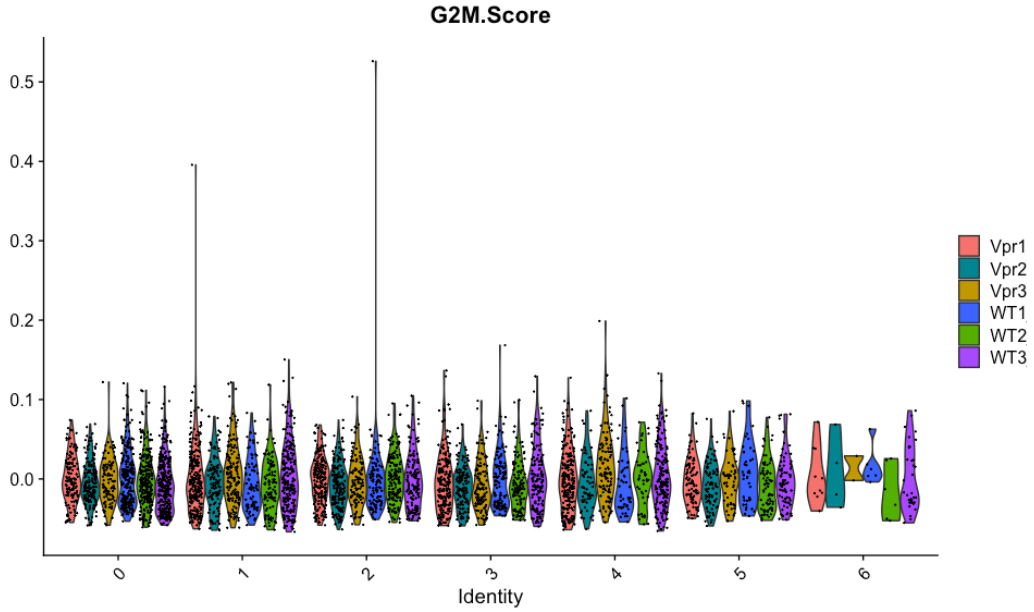

(c)

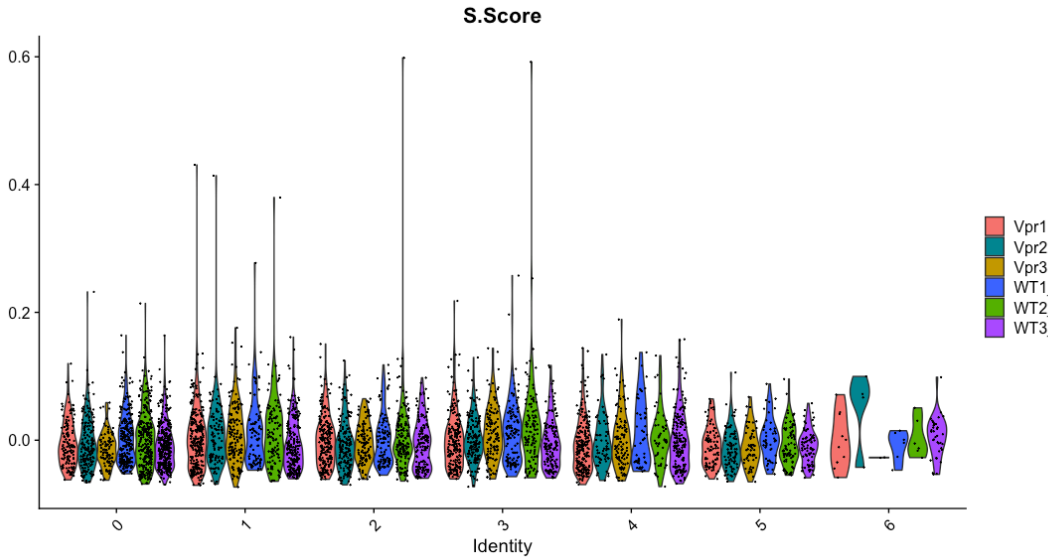

Supplementary Figure 6. Violin plots showing the aggregate gene scores of cell cycle genes in distal tubular cell subclusters. (a) G2M scores of 48 G2M phase genes (b) S scores of 40 S phase genes. Subcluster 0 = DCT1; subcluster 5 = DCT2; subcluster 6 = *Nr3c2*$^{+}$ DCT.

Cluster	**WT1**	**WT2**	**WT3**	**Vpr1**	**Vpr2**	**Vpr3**
Podocyte	0.39	0.44	0.37	0.44	0.05	0.13
MC	0.11	0.37	0.19	0.17	0.30	0.01
Cortical EC	13.68	14.11	9.49	10.78	12.86	12.65
Vascular EC	1.49	1.51	1.85	1.83	1.56	2.34
Fibroblast	4.22	3.53	2.96	3.11	4.89	2.80
SMC	0.26	0.33	0.44	0.50	0.20	0.40
Macula Densa	0.23	0.27	0.19	0.27	0.22	0.37
PT-S1	10.80	10.26	9.96	8.93	13.06	8.22
PT-S1/S2	14.37	14.57	14.99	14.49	21.96	13.34
PT-S2	22.34	20.05	11.00	11.52	16.13	14.12
PT-S2/S3	5.93	5.43	5.27	6.34	2.84	6.37
PT-S3	3.43	2.02	3.91	2.40	1.75	2.56
PT-S1_UK	0.95	1.25	0.73	1.30	0.55	1.49
Glyco	1.29	2.61	4.89	5.62	6.69	2.86
tDL	0.39	0.33	3.00	2.41	0.16	2.06
TAL-1	4.03	4.46	13.69	13.20	2.69	13.38
TAL-2	1.39	1.71	2.54	2.72	1.15	2.74
DCT	**3.58**	**4.30**	**3.67**	**1.86**	**2.86**	**2.36**
CNT	2.94	3.84	3.00	3.53	3.57	3.77
PC	1.76	2.11	3.33	2.87	2.03	3.29
IC-A	1.16	1.31	1.92	1.38	0.51	1.77
IC-B	0.88	1.43	1.16	1.26	1.43	1.49
Immune	2.44	2.55	0.99	2.51	1.24	1.09
T	1.18	0.68	0.22	0.50	0.39	0.21
Mito	0.76	0.53	0.25	0.05	0.92	0.18
DCT subclusters						
DCT1	**3.03**	**3.41**	**2.87**	**1**	**1.93**	**1.47**
DCT2	0.58	1.02	0.68	0.64	0.95	0.83
Nr3c1^{+} DCT	0.08	0.08	0.31	0.07	0.04	0.03

Supplementary Table 1. Metrics of the 25 cells clusters and 3 DCT sub-clusters that were identified in the unsupervised clustering of six mouse renal cortex samples. The percentage of individual cell type cells in each sample was calculated from the total number of cells from that sample. MC mesangial cell; Cortical EC = cortical endothelial cell; Vascular EC = vascular endothelial cell; SMC = smooth muscle cell; PT = proximal tubule; Glyco = Cells with high expression of glycolytic enzymes; tDL = thin descending segment; TAL = thick ascending limb; DCT = distal convoluted tubule; CNT = connecting tubule; PC = principal cell; IC = intercalated cell; T = T cell; Mito = mitochondria-enriched cell.

Variant Id	SNP Id	P-Value	NES	Tissue
chr16_56715244_C_T_b38	rs11649088	3.80E-05	-0.27	Spleen
chr16_56717614_G_T_b38	rs9932268	3.90E-06	-0.45	Spleen
chr16_56718282_C_CA_b38	rs34867225	9.80E-07	0.33	Spleen
chr16_56719719_C_T_b38	rs12931136	1.10E-06	0.32	Spleen
chr16_56721606_A_G_b38	rs12923723	2.80E-06	0.32	Spleen
chr16_56723904_A_G_b38	rs4783955	2.50E-05	0.27	Spleen
chr16_56729100_A_T_b38	rs9939873	2.50E-05	-0.28	Spleen
chr16_56730563_A_G_b38	rs4784726	4.20E-06	0.35	Spleen
chr16_56732919_C_T_b38	rs4783956	2.60E-05	0.28	Spleen
chr16_56733179_G_A_b38	rs12934065	1.10E-06	0.32	Spleen
chr16_56733213_T_A_b38	rs12921489	1.10E-06	0.32	Spleen
chr16_56733890_C_T_b38	rs12921698	1.10E-06	0.32	Spleen
chr16_56737879_T_C_b38	rs62036970	3.10E-05	0.28	Spleen
chr16_56746479_T_C_b38	rs12930689	2.60E-05	0.28	Spleen
chr16_56751211_C_A_b38	rs73555563	3.90E-06	-0.45	Spleen
chr16_56754842_G_A_b38	rs12930414	1.10E-06	0.32	Spleen
chr16_56758087_T_G_b38	rs12924698	3.40E-05	0.25	Spleen
chr16_56766421_T_A_b38	rs8048885	1.10E-06	-0.32	Spleen
chr16_56768702_TA_T_b38	rs564962218	1.90E-07	-0.73	Spleen
chr16_56774700_T_C_b38	rs4371151	2.80E-05	-0.27	Spleen
chr16_56775541_AG_A_b38	rs60454311	4.00E-05	-0.27	Spleen
chr16_56777549_A_C_b38	rs9928890	3.90E-06	-0.45	Spleen
chr16_56780935_G_A_b38	rs8052978	1.50E-05	-0.26	Spleen
chr16_56784635_T_G_b38	rs6499852	6.60E-07	-0.33	Spleen
chr16_56785259_T_G_b38	rs6416772	6.60E-07	-0.33	Spleen
chr16_56786728_G_A_b38	rs7500207	1.60E-05	-0.28	Spleen
chr16_56792854_T_C_b38	rs9938953	6.40E-07	-0.3	Spleen
chr16_56794811_C_T_b38	rs13335111	4.00E-05	-0.27	Spleen
chr16_56795628_G_A_b38	rs12932037	1.50E-05	0.29	Spleen
chr16_56796867_G_C_b38	rs10048067	1.50E-05	0.29	Spleen
chr16_56797234_C_T_b38	rs9922951	4.00E-05	-0.27	Spleen
chr16_56798390_C_T_b38	rs9927884	3.90E-06	-0.45	Spleen
chr16_56800184_A_G_b38	rs4783959	2.60E-06	-0.28	Spleen
chr16_56801800_G_T_b38	rs8051691	4.00E-05	-0.27	Spleen
chr16_56802196_T_C_b38	rs9929577	5.20E-06	-0.27	Spleen
chr16_56804675_G_A_b38	rs7189328	1.60E-05	0.28	Spleen
chr16_56805066_T_G_b38	rs13338063	4.70E-05	-0.25	Spleen
chr16_56806259_A_G_b38	rs7187512	8.40E-07	-0.29	Spleen

chr16_56806416_G_A_b38	rs10221121	1.30E-05	0.29	Spleen
chr16_56807802_C_T_b38	rs9938980	2.60E-05	-0.25	Spleen
chr16_56810727_TACCAGCGCCCCAGAAATCCTCTTTGTGGTCCTTTCTGGTC_T_b38	rs141700288	1.70E-06	0.33	Spleen
chr16_56811388_A_T_b38	rs72786721	1.90E-07	-0.73	Spleen
chr16_56812624_T_C_b38	rs12925122	6.60E-07	0.33	Spleen
chr16_56813358_G_A_b38	rs1529928	1.70E-06	0.33	Spleen
chr16_56815584_G_A_b38	rs1529929	8.40E-07	-0.29	Spleen
chr16_56816611_A_G_b38	rs13338782	3.90E-06	-0.45	Spleen
chr16_56816690_A_G_b38	rs9939678	8.40E-07	-0.29	Spleen
chr16_56818477_T_C_b38	rs12928581	1.60E-05	0.28	Spleen
chr16_56818910_G_T_b38	rs1561139	1.20E-06	-0.29	Spleen
chr16_56820372_C_T_b38	rs12930486	1.60E-05	0.28	Spleen
chr16_56825304_C_T_b38	rs12919839	1.50E-05	0.29	Spleen
chr16_56825683_G_A_b38	rs7199480	8.40E-07	-0.29	Spleen
chr16_56828083_C_G_b38	rs2099536	3.70E-07	-0.3	Spleen
chr16_56828231_GA_G_b38	rs34735016	3.70E-07	-0.3	Spleen
chr16_56830486_C_T_b38	rs1561140	5.20E-05	-0.25	Spleen
chr16_56830706_C_T_b38	rs4461062	8.40E-06	-0.27	Spleen
chr16_56831337_C_A_b38	rs4784730	8.40E-06	-0.27	Spleen
chr16_56832590_T_C_b38	rs12918918	6.60E-07	0.33	Spleen
chr16_56832889_G_T_b38	rs6499853	1.10E-06	0.32	Spleen
chr16_56834788_A_G_b38	rs1347591	1.20E-05	-0.27	Spleen
chr16_56836171_G_GT_b38	rs35892526	3.00E-06	0.31	Spleen
chr16_56837557_TTTTATTGATTAC_T_b38	rs145442551	3.90E-06	-0.45	Spleen
chr16_56838810_C_T_b38	rs3764265	3.90E-06	-0.45	Spleen
chr16_56840285_G_A_b38	rs1865830	8.40E-07	-0.29	Spleen
chr16_56840945_C_T_b38	rs2007432	8.40E-07	-0.29	Spleen
chr16_56841360_A_AT_b38	rs3214653	8.40E-07	-0.29	Spleen
chr16_56845290_T_C_b38	rs12918087	9.80E-06	0.33	Spleen
chr16_56845659_G_C_b38	rs7205421	3.60E-07	0.3	Spleen
chr16_56845726_G_C_b38	rs35172527	3.60E-06	0.31	Spleen
chr16_56846187_GATCACC_G_b38	rs147271366	1.40E-06	0.31	Spleen
chr16_56846246_A_G_b38	rs2399562	3.90E-07	-0.3	Spleen
chr16_56846493_T_C_b38	rs12929119	1.40E-06	0.31	Spleen
chr16_56846969_AGGTTCTTTGACCTGTAGATG_A_b38	rs144725437	1.40E-06	0.31	Spleen
chr16_56848952_AAG_A_b38	rs72067847	9.80E-06	0.33	Spleen
chr16_56849526_G_A_b38	rs8044753	5.50E-05	-0.25	Spleen
chr16_56849797_G_C_b38	rs8045306	8.40E-07	-0.29	Spleen

chr16_56850012_A_G_b38	rs735144	8.40E-07	-0.29	Spleen
chr16_56851226_T_G_b38	rs6499855	7.10E-06	-0.27	Spleen
chr16_56854080_G_A_b38	rs76942671	1.90E-07	-0.73	Spleen
chr16_56856531_C_CA_b38	rs35810185	6.00E-05	0.3	Spleen
chr16_56860192_T_C_b38	rs12933363	4.00E-06	0.3	Spleen
chr16_56860593_G_T_b38	rs12932041	3.00E-06	0.31	Spleen
chr16_56861122_G_T_b38	rs1436424	6.30E-07	-0.3	Spleen
chr16_56862124_T_C_b38	rs12599065	7.80E-07	-0.3	Spleen
chr16_56862277_A_G_b38	rs12921781	2.30E-06	0.31	Spleen
chr16_56862818_G_A_b38	rs3829502	9.70E-08	-0.32	Spleen
chr16_56866607_C_T_b38	rs12918664	3.20E-06	0.29	Spleen
chr16_56871338_C_T_b38	rs1123507	2.10E-13	-0.68	Spleen
chr16_56871338_C_T_b38	rs1123507	2.50E-06	-0.33	Small Intestine - Terminal Ileum
chr16_56873040_CT_C_b38	rs55822178	2.20E-12	-0.64	Spleen
chr16_56873040_CT_C_b38	rs55822178	2.50E-05	-0.31	Small Intestine - Terminal Ileum
chr16_56893416_A_C_b38	rs28728226	3.40E-05	0.32	Pancreas
chr16_56893529_G_C_b38	rs16963397	3.40E-05	0.32	Pancreas
chr16_56893808_T_C_b38	rs12449167	3.40E-05	0.32	Pancreas
chr16_56893846_C_A_b38	rs12445576	3.30E-05	0.32	Pancreas
chr16_56894038_C_T_b38	rs12445625	3.30E-05	0.32	Pancreas
chr16_56894148_T_C_b38	rs12449249	3.40E-05	0.32	Pancreas
chr16_56894165_A_G_b38	rs12448598	3.30E-05	0.32	Pancreas
chr16_56894270_G_A_b38	rs12445505	3.30E-05	0.32	Pancreas
chr16_56894304_C_T_b38	rs12445698	3.30E-05	0.32	Pancreas
chr16_56894368_G_C_b38	rs13306679	3.30E-05	0.32	Pancreas
chr16_56894763_C_A_b38	rs2289118	3.30E-05	0.32	Pancreas
chr16_56894793_A_C_b38	rs9921308	3.30E-05	0.32	Pancreas
chr16_56895768_G_T_b38	rs13338222	3.00E-05	0.32	Pancreas
chr16_56895929_T_C_b38	rs13334864	3.70E-05	0.32	Pancreas
chr16_56895989_A_G_b38	rs9929395	3.10E-05	0.32	Pancreas
chr16_56896007_C_T_b38	rs9939276	3.00E-05	0.32	Pancreas
chr16_56896008_T_G_b38	rs9931565	3.10E-05	0.32	Pancreas
chr16_56896317_G_T_b38	rs8056954	3.00E-05	0.32	Pancreas
chr16_56896339_T_C_b38	rs8063291	2.20E-05	0.33	Pancreas
chr16_56896519_A_G_b38	rs8063278	3.00E-05	0.32	Pancreas
chr16_56896638_G_A_b38	rs8061631	5.80E-06	0.34	Pancreas

chr16_56896723_G_A_b38	rs8061810	3.00E-05	0.32	Pancreas
chr16_56896753_T_A_b38	rs8047432	3.00E-05	0.32	Pancreas
chr16_56897008_T_C_b38	rs34589259	2.70E-05	0.32	Pancreas
chr16_56897136_G_C_b38	rs16963412	2.70E-05	0.32	Pancreas
chr16_56897409_A_G_b38	rs12923922	2.70E-05	0.32	Pancreas
chr16_56897553_T_A_b38	rs12447990	5.80E-06	0.34	Pancreas
chr16_56897653_C_T_b38	rs7188963	5.80E-06	0.34	Pancreas
chr16_56897792_G_A_b38	rs7187932	1.10E-05	0.33	Pancreas
chr16_56898410_T_C_b38	rs13338836	1.10E-05	0.33	Pancreas
chr16_56898619_G_A_b38	rs34433002	1.10E-05	0.33	Pancreas
chr16_56899308_A_G_b38	rs12448372	1.10E-05	0.33	Pancreas
chr16_56901178_G_C_b38	rs6499857	3.40E-05	0.31	Pancreas
chr16_56904610_C_T_b38	rs2289114	8.90E-06	0.34	Pancreas
chr16_56933265_T_G_b38	rs72786778	5.50E-07	-0.83	Spleen
chr16_56933265_T_G_b38	rs72786778	9.10E-06	-0.43	Small Intestine - Terminal Ileum
chr16_57405846_A_T_b38	rs62037105	3.40E-05	-0.48	Lung
chr16_57407454_T_A_b38	rs60679405	3.40E-05	-0.48	Lung
chr16_57408777_T_C_b38	rs112186794	3.40E-05	-0.48	Lung
chr16_57409259_G_A_b38	rs62037108	3.10E-05	-0.48	Lung
chr16_57410859_A_G_b38	rs62037110	1.80E-05	-0.53	Lung
chr16_57414449_T_C_b38	rs59247888	3.40E-05	-0.48	Lung
chr16_57415695_CG_C_b38	rs149367659	3.40E-05	-0.48	Lung

Supplementary Table 2. Expression quantitative trait locus (eQTL) SNPs associated with *SLC12A3* expression levels across different tissues retrieved from the Genotype Tissue Expression (GTEx) database.

Anln
Anp32e
Aurka
Aurkb
Birc5
Bub1
Ccnb2
Cdc20
Cdc25c
Cdca2
Cdca3
Cdca8
Cenpa
Cenpe
Cenpf
Ckap2
Ckap2l
Ckap5
Cks1b
Cks2
Ctcf
Dlgap5
Ect2
G2e3
Gtse1
Hjurp
Hmgb2
Hmmr
Kif11
Kif20b
Kif23
Kif2c
Lbr
Mki67
Ncapd2
Ndc80
Nek2
Nuf2
Nusap1
Psrc1

Rangap1
Smc4
Tacc3
Top2a
Tpx2
Ttk
Tubb4b
Ube2c

Supplementary Table 3. The mouse G2M phase genes used to calculate aggregate gene scores shown in **Supplementary Figure 5a**.

Blm
Brip1
Casp8ap2
Ccne2
Cdc45
Cdc6
Cdca7
Chaf1b
Clspn
Dscc1
Dtl
E2f8
Exo1
Fen1
Gins2
Gmnn
Hells
Mcm2
Mcm4
Mcm5
Mcm6
Msh2
Nasp
Pcna
Pola1
Prim1
Rad51
Rad51ap1
Rfc2
Rpa2
Rrm1
Rrm2
Slbp
Tipin
Tyms
Ubr7
Uhrf1
Ung
Usp1
Wdr76

Supplementary Table 4. The mouse S phase genes used to calculate aggregate gene scores shown in **Supplementary Figure 5b.**